J. Earth Syst. Sci. (2020)129 71
https://doi.org/10.1007/s12040-020-1341-0

Groundwater exploration in limestone–shale–quartzite terrain through 2D electrical resistivity tomography in Tadipatri, Anantapur district, Andhra Pradesh

Dewashish Kumar*, Karri Rajesh, Setbandhu Mondal, Taufique Warsi and R Rangarajan

CSIR–National Geophysical Research Institute, Hyderabad, India.
**Corresponding author. e-mail: dewashishkumar@ngri.res.in*

MS received 26 July 2019; revised 22 November 2019; accepted 28 November 2019

Two-Dimensional (2D) Electrical Resistivity Tomography (ERT) survey was carried out at 11 sites within an area of 10 km^2 to delineate deeper potential groundwater zones in a complex geological terrain underlain by quartzite, shale and limestone formations with varied resistivity characteristics. The area is in medium rainfall zone in Tadipatri mandal of Anantapur district, Andhra Pradesh state, India. The investigation was carried out to meet the growing demands of water supply. Interpretation of the high-density 2D resistivity dataset results revealed potential zones at only three sites in Tummalapenta, Ayyavaripalle and Guruvanipalle villages within the depth zone of 24–124 m. A major fault zone oriented in EW direction is mapped at Tummalapenta site. Based on high resolution geophysical data interpretation and significant anomalies, four boreholes were drilled in complex, viz., limestone, shale and quartzite formations up to a maximum depth of 192 m in the area with the yield ranging from 300 to ∼5000 liter per hour (lph). These four anomalous drilled borehole sites corroborates with the aquifer zone delineated through ERT technique. The aquifer parameters estimated from pumping tests show that the transmissivity varies between ∼0.3 and 179.5 m^2/day while the storage coefficient ranges from 0.137 to 0.5 indicating large variation in aquifer characteristics of the system in a smaller area. Suitable water conservation measures were suggested for improving the groundwater condition and yield of the pumping wells.

Keywords. Electrical Resistivity Tomography; quartzite; shale–limestone formations; water scarcity areas.

1. Introduction

Groundwater exploration and prospecting in a complex sedimentary terrain comprising limestone–quartzite–shale formation is a crucial task for delineating potential groundwater zones. The problem multiplies in areas where seasonal rainfall is meager, and recharge rate is poor. Geophysical methods produce indirect evidence for favourable subsurface geological features and structures, which could hold water under the different hydrogeological conditions and thus become the potential water bearing zones.

The conventional electrical resistivity (direct current (DC)) methods were commonly used for groundwater exploration and prospecting using various electrode configurations such as Wenner, Schlumberger, dipole–dipole, pole–dipole, and

Published online: 15 February 2020

pole–pole arrays (Telford *et al.* 1976). The type of array depends largely on the objective of the work, the targets of interest, the local geology, and sensitivity of the array to vertical and lateral variations in the subsurface resistivity distribution of the rock matrix. Electrical resistivity surveys are deployed to distinguish various subsurface anomalies obtained from electrical resistivity contrasts. These resistivity contrasts are mainly associated with lithology and the hydrogeological characteristics of the earth's medium. The heterogeneous nature of overburden rock mass can be better understood by taking into account the maximum coverage of the electrical data in an area of study by acquiring 2D or 3D high-resolution electrical resistivity dataset. The effectiveness of the geoelectric resistivity method in producing high-resolution two- and three-dimensional resistivity models was greatly developed and enhanced in the last two decades by the application of the automatic data acquisition systems and the computer inversion codes (Loke and Barker 1996; Dahlin 2001). The emphasis and utility of dense data density sampling in electrical resistivity tomography survey (Dahlin and Loke 1998) has given a new dimension of research for groundwater exploration and prospecting in any geological medium.

A state of the art technique – Electrical Resistivity Tomography (ERT) being extensively used in groundwater exploration and prospecting, engineering geophysics areas and in environmental site investigations. It has evolved 2D and 3D high-resolution images of the subsurface resistivity characteristics in areas with complex geology and hydrogeology (Griffiths and Turnbull 1985; Griffiths *et al.* 1990; Barker 1992; Griffiths and Barker 1993; Dahlin 1996; Hossain 2000; Suzuki *et al.* 2000; Demanet *et al.* 2001; Daily *et al.* 2004; Adepelumi *et al.* 2006; Gokturkler *et al.* 2008; Andrade 2011; Robert *et al.* 2011; Abdulaziz *et al.* 2012; Kumar 2012, 2016a; Gupta *et al.* 2015; Balkaya *et al.* 2018; Thiagarajan *et al.* 2018; Swileam *et al.* 2019a, b). Geoelectrical method and its applications in environmental and hydrogeological investigations have many advantages, especially by its indirect and non-invasive characteristics. This property helps in delimiting the saturated water depth, identifying the groundwater flow direction in the study of contaminants in the subsurface geological strata (Ward 1990). Electrical imaging technique is based on the realization of the apparent resistivity measurements along a profile to carry out a systematic resistivity variations in one or more levels in depth (Ward 1990). Kumar *et al.* (2016a) in their work explained and discussed the high-resolution ERT and time-domain-induced polarization (TDIP) datasets over a granitic terrain to provide safe and sustainable drinking water in a severe water scarcity area of Telangana, South India. In another scientific study, Kumar *et al.* (2016b) used high-resolution ERT data in delineating depth of soil layer, highly weathered, moderately weathered zones and deeper massive granites and established the correlation of the various subsurface geological strata with the borehole lithology in a hard rock aquifer system. The examination and exploration of the complex geology and poorly stratified lateritic overburden rock mass was tested and verified by the electrical resistivity tomography (Griffiths and Barker 1993; Ritz *et al.* 1999; Pucci *et al.* 2016; Thiagarajan *et al.* 2018). In yet another study, 2D resistivity profiles indicated remarkably different geostratigraphic units of Bijawer and the Bundelkhand granite aquifer system, Madhya Pradesh. The drilled boreholes have shown a good match between the resistivity tomograms and the lithology of the boreholes (Singh and Paramasivam 2016) for groundwater prospecting. Nevertheless, the unit electrode spacing is the key factor, which affects the length of the profile, the penetration depth and the resolution of the subsurface features (Ritz *et al.* 1999) for a given electrical resistivity model. Aizebeokhai and Oyeyemi (2014) and Dahlin and Zhou (2006) showed in their work the significance of the multiple-gradient array and added with the advantage of measurement logistics as well as with the improved electrical image resolution of the subsurface geological features and structures over the Wenner array.

Seeing a real problem on the shortage of water – a geoscientific study was carried out in a cement mining and plant area in Tadipatri Mandal, Anantapur district, Andhra Pradesh, South India for a detailed exploration and prospecting as well as development of groundwater resources both at a shallow and the deeper depths. Another major concern in this area is the depletion of available groundwater resources in the aquifer system due to the discharge exceeding the recharge of the rain water to the groundwater table. It is thus essential to deploy high-resolution 2D electrical resistivity technique to visualize and map the subsurface hydrogeological scenario of the aquifer within the area of study. In the present work, we presented

high resolution ERT data acquisition and their results of the interpretation at five sites for detailed mapping the subsurface lithological formations, geological structure(s) and understanding the variation in resistivity in a complex geological settings of the study area. These interpreted results helped and delineated potential groundwater zones and subsequently identified few suitable sites for deep drilling up to the depth of 200 m for both shallow and deeper groundwater prospecting and development of the resource. In addition, we suggested a proper recharge measure for sustaining water supply from the existing and the newly drilled boreholes in and around the area of study.

2. Study area and geology

The study area (10 km^2), comprises cement plants (2 units), office and residential built-up areas, mining area, fallow pasture, rainfed land and agricultural areas. It is located at a distance of about 10 km north of Tadipatri town and 3 km west of Kolimigundla village, Anantapur district, Andhra Pradesh, South India (figure 1). The topographic elevation of the area ranges from a maximum 449 m amsl to a minimum 344 m above mean sea level (amsl), while the investigated area varies from 300–350 m amsl. The area is drought prone and falls under a semi-arid agro-climatic zone with an average annual rainfall of 670–700 mm. The area around the plant and mining is dry agricultural, barren or rocky terrain. The soil is black cotton, which is enriched with clay formed in regions (tropics and subtropics) having poor drainage conditions with a thickness of about 1–2 m. Topographically, the area is an undulating terrain and has hills in the eastern and western sides of the study region. The drainage is controlled by two smaller streams flowing from north and northeast to south and southwest directions. The area lies within Cuddapah geological basin. The regional geology as per King (1872) comprises Bairenkonda quartzite (older upper Cuddapah group) and Banganapalle quartzite, Narji limestone, Owk shale and Paniam quartzite (younger Kurnool group) as studied in this area. The limestone, which is the predominant rock, belongs to the Narji stage of Jammalmadugu series (Kumar *et al.* 2015). The strike of the formation is NW–SE and gently dips in E–NE and NE directions. The Narji limestone formation is having upper flaggy part followed by middle massive and compact limestone and lower one again the flaggy limestone formation. The basal flaggy limestone comprises thin bedded light gray or purple argillaceous limestones within the study area.

3. Hydrogeology

The study area constitute and underlain a complex hydrogeological setup. The principal water-bearing zones and formations comprise the Narji limestone and shales underlain by quartzites rock formation. It was found that occurrences and the movement of groundwater is controlled by the depth of weathered rocks mass (Kumar *et al.* 2015), the presence of bedding planes, fractures and faults and the existence of solution channels/cavities in a limestone formation. Groundwater is mainly extracted through the exploratory boreholes drilled through shale–quartzite weathered-fractured formations, which is under semi-confined conditions in this area, whose maximum depth is ∼200 m. The lithological information from the existing boreholes indicated that the aquifer is met within 15–46 m depth range and the yield of the boreholes varies between 1.5–2″, i.e., 35–72 m^3/d. Monitoring of the measured water levels from the four newly drilled boreholes within the study area vary from 6.2 to 23.0 m below ground level (bgl) during December 2015. This large variation in water levels suggests a change in groundwater dynamics as well as due to topography changes within the area. A natural storage structure in the western part of the study area receives inflow only during the high-intensity rainfall events or excess rainfall years. During the period of impoundment, the yield of the boreholes in the downstream of the area improves due to moderate to heavy recharge to the groundwater system, which shows the connectivity of the aquifer layers/zones with the recharge source in the area.

Eleven core lithology of the boreholes was available up to a maximum depth of 50 m, which indicated thin black soil zone followed by a hard compact gray limestone with some clay up to 10 m depth and subsequently followed by bedded cherty limestone up to 35 m depth. It was also seen from some of the core lithology, which indicated 2–3 m of loose boulders followed by flaggy limestone with clay up to 10 m depth, subsequently followed by massive gray limestone with fractures, clay lenses up to 40 m depth and further down by calcareous shale. No deeper information on geological strata was available in the study area. The area is a low

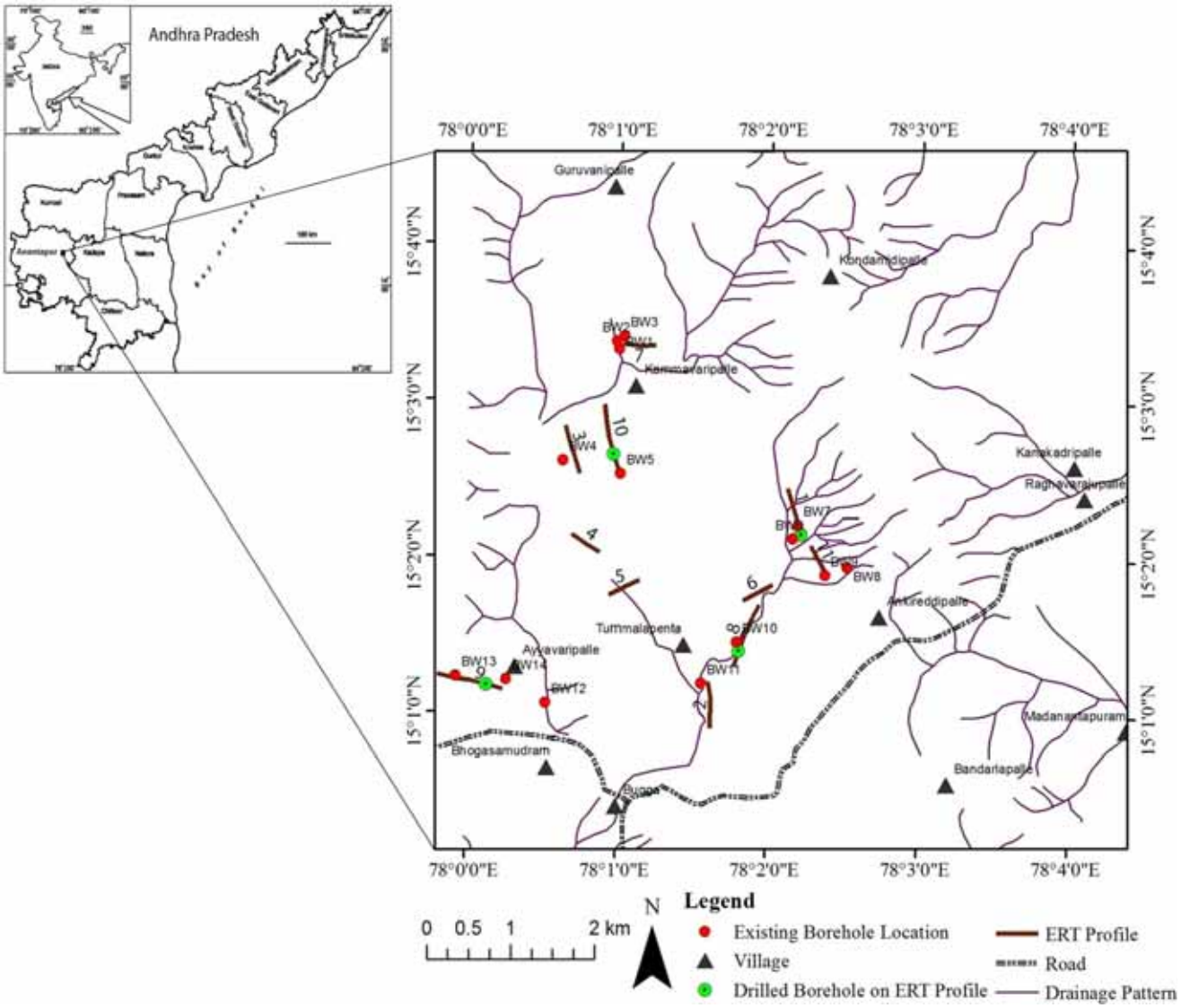

Figure 1. Depicted the study area with reference to the geographical map of India (source: GSI) and with the location of ERT profiles at 11 sites in the study area.

potential zone mainly due to lower rainfall and a poor recharge to the aquifer system. Twelve years of rainfall data during the period 2004–2015 indicated that it is below normal in 2013 and 2014 and a normal rainfall of 752 mm during the year 2015. The rainfall data also shows that annual rainfall is in declining trend since 2009. The seasonal rainfall (June–September) declined from 923 mm in 2009 to 276 mm in 2014. The daily rainfall pattern since 2004, shows that in each year there are few rainfall events of greater than 30 mm/day, which cause runoff events in the area. It was also observed that the one-day daily event of 80 mm occurred in July 2015. The high-intensity rainfall event during July to October 2015 has generated a significant runoff, which causes the large storage of rainfall water in the two mine pits area. Also, it was found that the

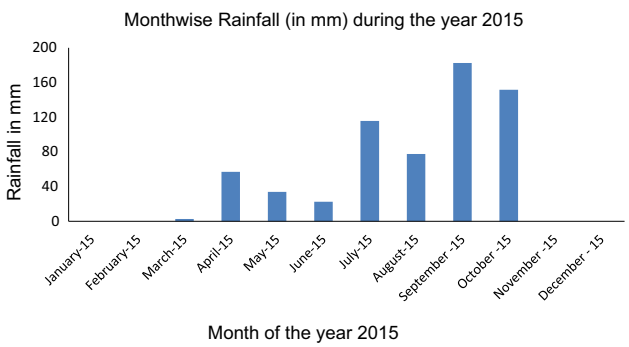

Figure 2. Monthly rainfall variation during the year 2015 within the study area.

groundwater levels at the newly drilled boreholes show marginal improvement after the high-intensity rainfall events during the year 2015 (figure 2).

4. Materials and methods

4.1 *Electrical resistivity tomography*

Two-dimensional (2D) ERT technique is universally deployed in mapping the subsurface rock strata, geological structure and lineaments, lithology for groundwater exploration and prospecting and other geoscientific studies due to its large range of resistivity values (Griffiths and Barker 1993; Hossain 2000; Pucci *et al.* 2016). Subsurface resistivity structure and distribution were estimated using standard inversion approach – least-squares smoothness constrained inversion algorithm (Loke and Dahlin 2002; Loke 2012a). Dahlin and Loke (1998) have established that the Gauss–Newton least-squares inversion approach is the most appropriate method as it gives more precise results than the quasi-Newton method in the inversion of 2D resistivity dataset with a large resistivity contrasts (Loke and Barker 1996). In the present work, we need both the large data density coverage as well as a better resolution to delineate deeper strata and minor hydrogeological subsurface features for exploration and prospecting of groundwater resources as well as its development. Due to the specific need for groundwater prospecting, we carried out ERT survey using the more appropriate configuration namely pole–dipole array for acquiring the optimal 2D apparent resistivity dataset. This pole–dipole configuration provides a good resolution of geological structures, larger depth of penetration within a limited electrode spread on the ground (Loke 2012b). In addition, it has a relatively good horizontal coverage on the ground as well as significantly higher signal strength but needs a remote current (C2) electrode, which must be placed at far-off distance from the geophysical survey line during the process of data acquisition. In the present investigation, a total of 1,040 to 1,332 apparent resistivity full waveform data points were collected for each site with either 41 or 81 electrodes, respectively (based on the availability of space in the field area) with an electrode spacing of 10 m, which were planted vertically into the ground and covered 11 sites with 6.0 km line in the study area (figure 1) by using 4 channel ABEM Terrameter LS system (ABEM 2012).

5. Depth of investigation (DOI) analysis

The depth of investigation in any direct current resistivity method of surface geophysical prospecting is defined, following Evjen (1938), as that depth at which a thin horizontal (parallel to ground surface) layer of ground contributes the maximum amount to the total measured signal at the ground surface (Roy and Apparao 1971). We can still define the depth of investigation unambiguously as that depth, which contributes most to the total signal measured on the ground surface. The depth of investigation in any electrode system is determined by the positions of both the current and the potential electrodes and not by the current penetration or distribution alone (Roy and Apparao 1971). It generally varies between 1/3 and 1/5 of the array length (i.e., the maximum length of the transmitting current, AB electrodes) in a geophysical survey. It also highly depends on the geology of the area (i.e., resistivity or conductivity of the subsurface geological formations), the acquisition array geometry, and of course data error *if any* (Oldenburg and Li 1999).

5.1 *Parameters controlling the depth of investigation (DOI)*

The larger the length of the transmitting current (AB) electrodes, the deeper the penetration of the current, the farther the M, N receiving potential electrodes from the AB, the more representative the potential measured on the surface of the ground, of the resistivity of deep layers (Bernard 2003). Practically, the depth on investigation (DOI) also depends on the measurability of the V_{MN} potential, which can be expressed as $V_{MN} = \rho \times I_{AB}/K$. For large investigation depths, the electrodes (AB) have to be far away from each other, K is the geometrical coefficient of the array, ρ is the resistivity and $I_{\mathbf{AB}}$ is the current, potential V_{MN} signal for deeper depths becomes small, which we can overcome by using a high current transmission for optimal output power transmitted into the ground, here in our present study, we use 250 W powerful equipment ABEM Terrameter LS (ABEM make). We used pole–dipole array in the present survey for deeper investigation (Loke 2012a); which has a good resolution of geological structure from a multi-channel data acquisition system (ABEM make).

6. Results

6.1 *Interpretation of 2D electrical resistivity tomography models*

Two-dimensional (2D) inverted model results of the resistivity tomograms provided the detailed

subsurface resistivity information showing a large variation in resistivity values from ∼20 to 2.75×10^5 Ωm, which indicated both the conductive and the resistive rock formations with a large variation in resistivity up to the maximum depth of 230 m. As the existing lithology data is only available down to 50 m depth, the calibration and correlation with the resistivity models is limited to shallow depths. There are few deep boreholes up to 200 m that exists in the area, but their lithology information is not available. This made us much more curious to investigate in detail the deeper rock strata in such a complex geological setting from near surface layers to the deeper 200 m depths. Based on the resistivity tomograms result from the subsurface formations and their hydrogeological interpretation, five sites were selected and recommended for deep borehole drilling in the investigated area. The sites are: (i) Tummalapenta (site-1), (ii) near Kona Venkateshwara Temple (site-2), (iii) Tummalapenta (site-8), (iv) Ayyavaripalle (site-9), and (v) Guruvanipalle (site-10). These five sites are hydrogeologically found quite favourable for groundwater prospects and development from shallower to deeper depths as per the detailed interpretation of 2D resistivity results. It is studied that the high-resolution and large density resistivity dataset helped immensely for the hydrogeological interpretation (Kumar 2012) in a different geological terrain. In our present study, we achieved high resolution resistivity models of the subsurface geological strata. The modelled resistivity value inferred for aquifer ranges from ∼15 to 250 Ωm at various depths. However, the detailed interpretation and results of five ERT sites/profiles are presented in this paper, which indicated and delineated the prospective groundwater scenario, highly resistive and conductive zone(s), weathered/fractured geological strata, deep fault structure and the massive rock(s) based on the resistivity values and their contrast in the complex and varied geological settings of the area.

6.2 *Site-1 and 8*

Two-dimensional inverted resistivity model at Tummalapenta (site no. 1) is laid in NS direction (figure 3a) on the eastern side of the area. The model resistivity section shows a low resistivity zone with a resistivity between ∼20–150 Ωm towards the southern side of the section. A major fault (**F–F**) is seen and mapped from the modelled resistivity section, which separates the low resistivity (100–200 Ωm) and a high resistivity (>17×10^3 Ωm) zone with a sharp resistivity contrast right below 320 m lateral distance. The inferred fault is very deep (>200 m) and is extended up to a depth of 230 m as revealed from resistivity section (figure 3a). The resistivity of the geological formation towards the north of the fault (**F–F**) is very high >17×10^3 Ωm, which suggests such area is entirely devoid of groundwater as the formation is highly resistive and massive. The potential target for groundwater prospecting is therefore limited to the southern side and region near the fault zone (figure 3a). The geological implication of the model with reference to 2D resistivity model at site-1 describing the detailed geological sequence of rocks from near surface layer to the depths is presented here (figure 3b). It shows the detailed geological tectonic setup and the hydrogeological variation all along the fault zone. This model depicted the main fault structure, the weathered and fractured limestone, shale and quartzite zones all along the fault, various types of limestone, shale, weathered quartzite and the thick massive quartzite rock towards the north of the fault plane. The borehole drilled up to 154 m depth encountered water in pink shale and weathered quartzite at a depth of 124 m (figure 3a), which is under confined condition within the subsurface. The implication of this model suggests the hydrogeological scenario as well as delineated major fault zone mapped through high resolution electrical tomography, which is the main target for groundwater exploration and development and is the major source for groundwater in the present geological setting. But towards the north, the thick massive quartzite rock is totally devoid for groundwater prospecting as seen from the geological model (figure 3b).

The another unique 2D inverted resistivity model in Tummalapenta (site no. 8) inferred groundwater potential zone towards the SW direction (figure 4a) between lateral distances 500–640 m in the depth range 110–180 m. The resistivity of this potential groundwater zone ranges between ∼100–450 Ωm. This inferred groundwater zone is overlain by comparatively hard geological formation with a variable resistivity values from 450–5000 Ωm. Towards the NE side, the resistivity modelled data indicated the hardest geological formation within the depth section of 34–150 m. This is continuing further down with a gap of slightly low resistivity, till the bottom 230 m depth (figure 4a). The geological model depicted shale, saturated shale, shale and saturated quartz

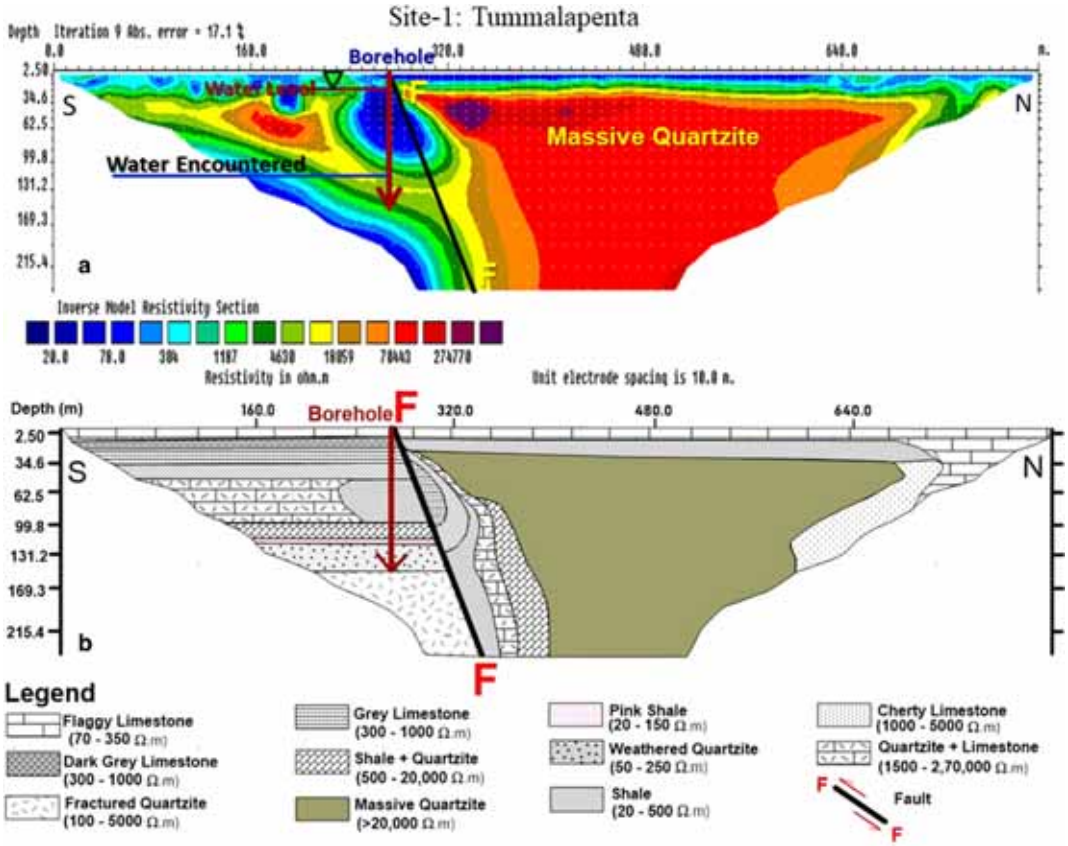

Figure 3. (**a**) 2D inverted resistivity model at site-1, which shows a large resistivity contrast, delineated a major fault (**F–F**) structure and the groundwater potential zone towards the southern side near the fault; **(b)** depicted the geological model, main fault structure, borehole and the thick massive quartzite rock towards the north of the fault plane.

vein, weathered and saturated shale, saturated shale and quartzite and shale and quartzite formations (figure 4b) based on the resistivity results and their variation (figure 4a). The conceptual geological model was achieved based on 2D resistivity model result, its interpretation and the lithology information collected from the drilled borehole at this site. The borehole encountered kankar, shale, saturated shale, shale and saturated quartz vein, weathered and saturated shale and saturated shale and quartzite up to a depth of 192 m (figure 4b). Water encountered in saturated shale at 24 m depth. The implication from the geological model confirmed and illustrates the water encountered in saturated shale at 24 m depth, which is underlain by shale and saturated quartz vein, followed by weathered and saturated shale and then the saturated shale and quartzite at the deeper depth. The saturated shale and quartzite is the main source for groundwater exploration, prospecting and development at a deeper 192 m depth. The model resistivity values for the various litho units achieved from the borehole lithology are corroborating with the conceptual geological model (figure 4b) for its hydrogeological significance.

6.3 *Site-2*

Inverted resistivity 2D model oriented along N–S direction is depicted in (figure 5a), which is located in southern part of the study area (figure 1). The resistivity model shows a heterogeneous subsurface scenario of the geological formation showing a large variation in resistivity from near surface layers to the deeper depths. The near surface layer shows a low resistivity <200 **Ω**m up to a depth of 20 m especially in northern side of the resistivity section (figure 5a). A low resistivity geological formation 20–300 **Ω**m revealed at a depth of 60–80 m lying at a lateral distance between 95 and 230 m, which is dipping towards north is inferred as prospect groundwater zone. This low resistivity zone seems to be connected to the near surface recharge source in the southern side of the resistivity section (figure 5a). Above

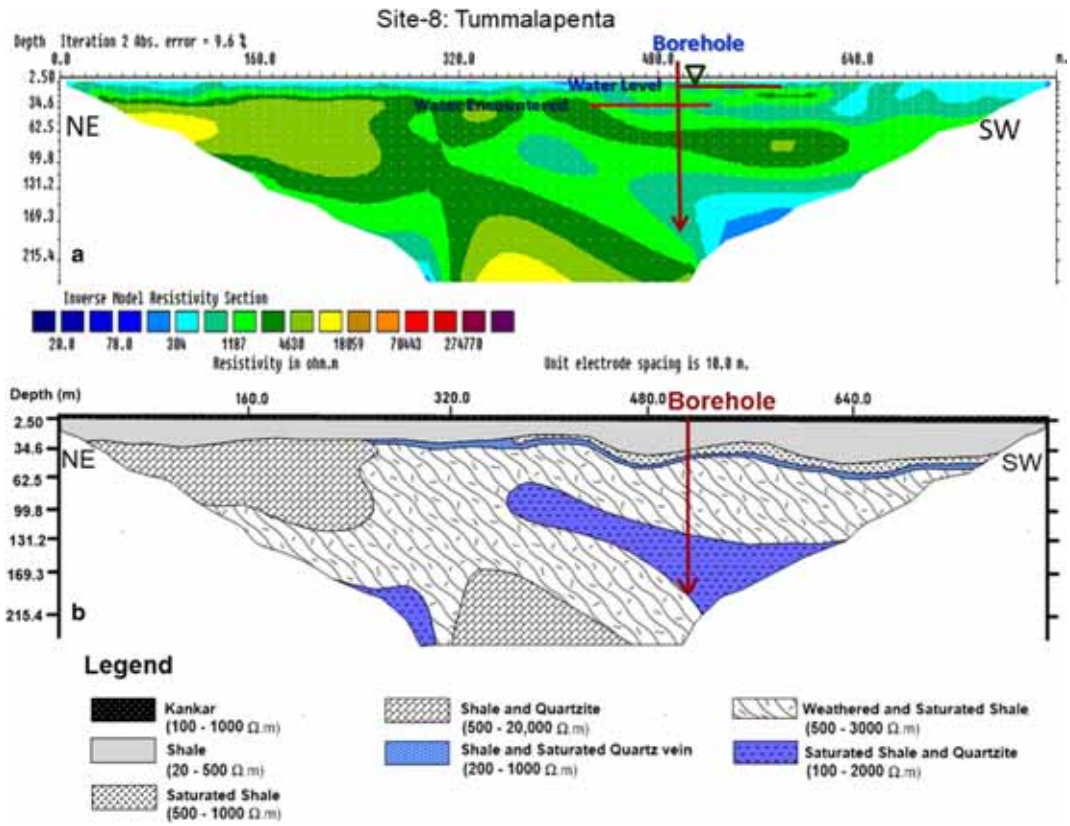

Figure 4. **(a)** Depicted a 2D inverted resistivity model at site-8 with a high resistivity towards the NE side and a potential zone for groundwater exploration in SW, which is confirmed by a drilled borehole at 510 m lateral distance; **(b)** conceptual geological model based on the 2D resistivity result depicting borehole encompasses shale, quartzite and saturated shale and quartzite formation in the entire geological strata up to 192 m depth.

and below this low resistivity zone lies in a very high resistivity geological formation up to depth of ∼25 and ∼170 m, respectively, which is totally devoid of prospect groundwater zone as revealed from the resistivity model result (figure 5a). The geological model (figure 5b) based on the resistivity result (figure 5a) depicted near surface saturated shale and quartzite, weathered and saturated shale formation and shale and quartzite formation (figure 5b). The saturated shale and quartzite formation is the characteristics of the prospect groundwater zone, which is inferred from the resistivity values and their contrast at this site.

6.4 *Site-10*

Two-dimensional inverted resistivity model at Guruvanipalle (site no. 10) oriented in NS direction clearly inferred groundwater potential zone towards the south of the resistivity section (figure 6). The 2D entire resistivity section shows a large resistivity contrast ranging from ∼10 to ∼70×10^3 Ωm (figure 6). The near surface layer constitutes low to medium resistivity formations, which depicts heterogeneity and where resistivity values range between 100–2000 Ωm all along the profile. Towards the southern side and between lateral distance 480–640 m of the inverted resistivity model, a prospect groundwater zone is inferred (figure 6) where the formation resistivity ranges between ∼15 and 150 Ωm (figure 6). This groundwater zone is prominent at ∼35 m depth and continues beyond 200 m depth, and its dimension is increasing from close to near surface layers to the deeper depths with a resistivity contrast of ∼200 Ωm. The inverted resistivity model shows subsurface geological formation and its structure is entirely different in northern part than in the southern part of the resistivity section (figure 6). Based on the resistivity result and its variation, the subsurface formation is highly weathered, fractured and saturated in the southern part, while it is the hardest formation and devoid of water bearing in the northern side of the resistivity section (figure 6).

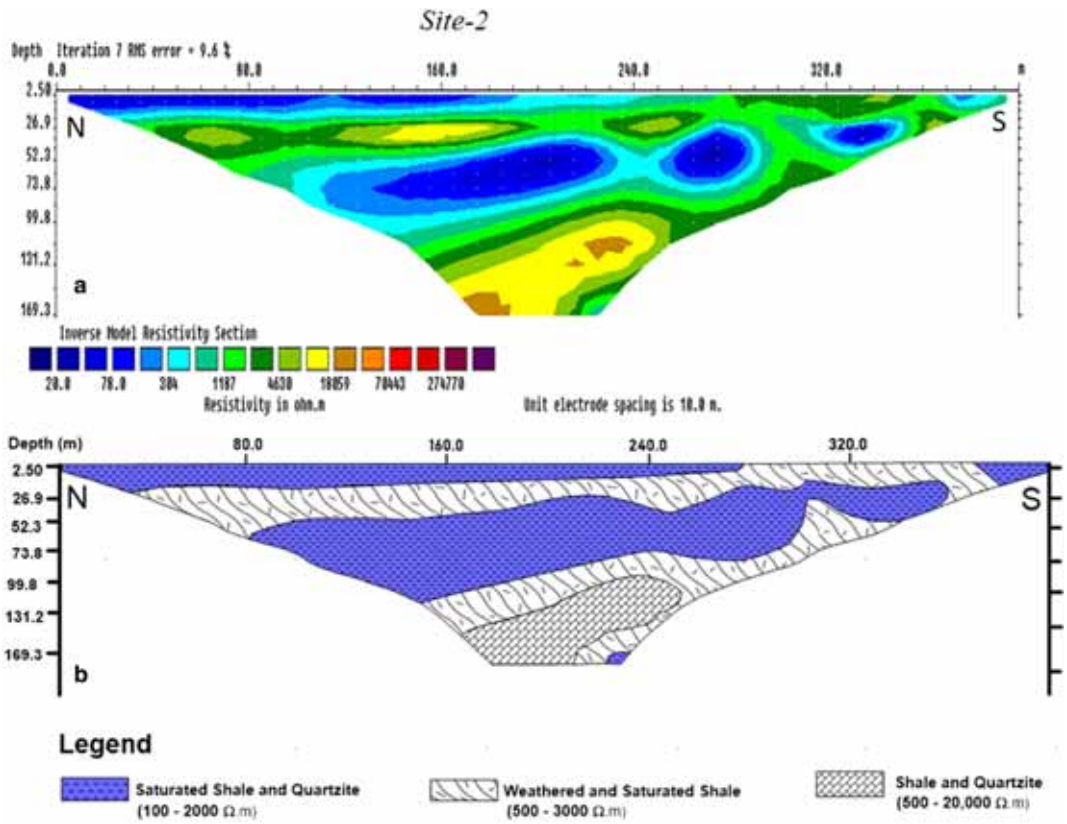

Figure 5. (**a**) Depicted a 2D inverted resistivity model at site-2, which revealed a heterogeneous subsurface of the geological formation with a large range of resistivity variation from the near surface layers to depths; (**b**) depicted the geological model based on the resistivity result, which revealed a prospect groundwater zone in saturated shale and quartzite formation.

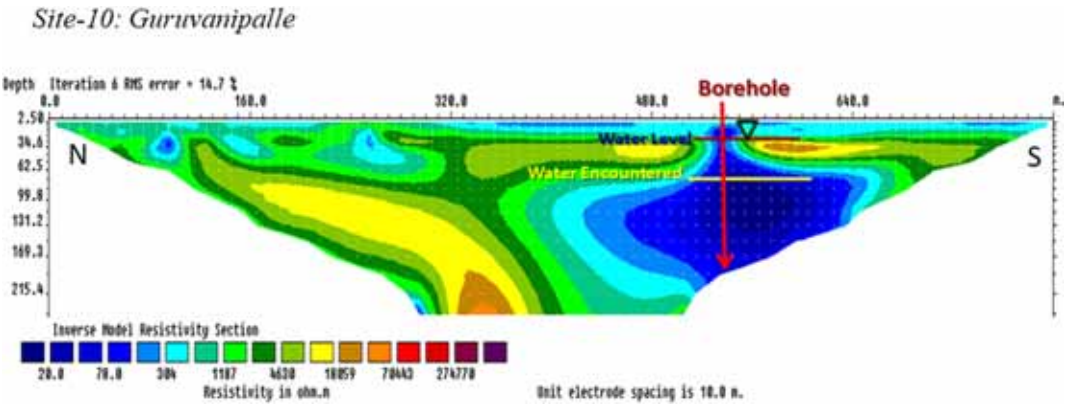

Figure 6. 2D inverted resistivity model at site-10 shows a potential groundwater zone towards southern side, which is confirmed by a drilled borehole at 535 m lateral distance. The high resistivity massive formation is delineated from 35 to 230 m towards northern side of the section with no prospect for groundwater exploration.

6.5 *Site-9*

Inverted 2D resistivity model at Ayyavaripalle (site no. 9) is located in the topographically low-lying area towards the west of the study area (figure 1). It is oriented along EW direction. The model resistivity structure shows comparatively a better prospect scenario in the eastern direction than in the western side of the section (figure 7a). The subsurface geological formation is more weathered towards the eastern side with a resistivity contrast >300 **Ω**m up to 100 m depth. The high resistivity indicated the hard and massive formation with a different degree of compactness and hardness showing the resistivity value in the range ∼300 to 18×10^3 **Ω**m (figure 7a). The

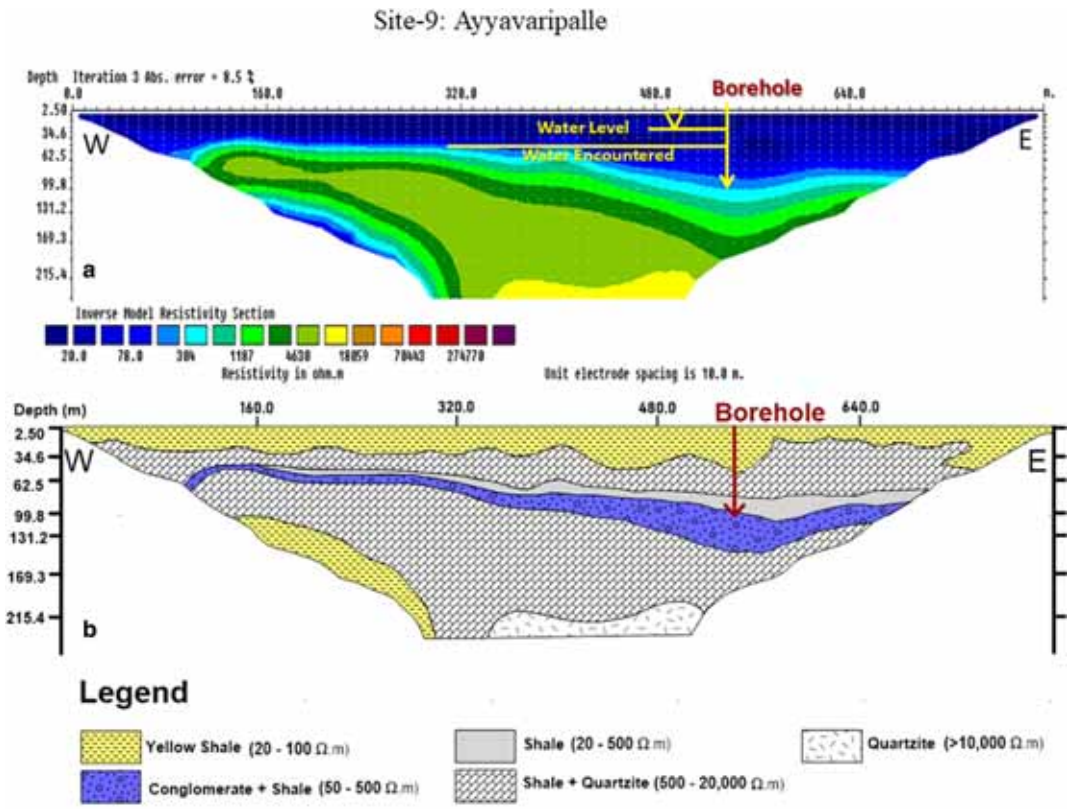

Figure 7. (**a**) 2D inverted resistivity model at site-9 showing low resistivity at near surface layers followed by high resistivity until the bottom depth of the section, a high yielding borehole was drilled towards eastern side of the section; **(b)** conceptual geological model depicting shale, quartzite and conglomerate formation. The borehole encompasses shale, shale and quartzite, thin shale layer as well as conglomerate and shale layer up to 81 m depth.

groundwater prospect zone lies at a shallower depth between 30–100 m depth on the eastern side of the resistivity model (figure 7a) with a resistivity ∼15 to <100 **Ω**m and is located between 540–620 m lateral distance towards the east of the resistivity model (figure 7a). This is hydrogeologically the most favourable site for groundwater prospecting and development compared to other part of the resistivity section. The conceptual geological model revealed different types of shale, conglomerate and quartzite formation (figure 7b). The thin layer of conglomerate imparts an idea about the surface of erosion and non-deposition. Since this site is lying in the downstream side of the area, it is devoid of tectonic activity. This resulted in more stratified geological layers compared to other four sites. This scenario is revealed in the conceptual geological model. The borehole encountered shale, shale and quartzite, and shale and conglomerate up to a depth of 81 m (figure 7b). A layer of shale formation is sandwiched between thick shale and quartzite and the conglomerate and shale formation (figure 7b). Water encountered in shale and quartzite formation at a depth of 42 m. This model revealed shale and quartzite layer at a shallower depth towards west than in the east direction. The thickness of weathered zone is more towards the east of the profile than in the west (figure 7b), which is the most potential target for groundwater prospecting and development.

6.6 *Drilling of boreholes and validation of model results*

New drilling was accomplished at four sites based on 2D resistivity data interpretation, results and hydrogeological favourable conditions within the subsurface. All the four boreholes namely at site-1, 8, 9 and 10 encountered water during the drilling and tapped the aquifer zones, which is mainly at the contact zone(s) of shale and quartzite rocks as well as in the weathered shale formation (figure 8). The drilled point was exactly marked at the anomalous zones showing well defined resistivity contrast with respect to the surrounding geological

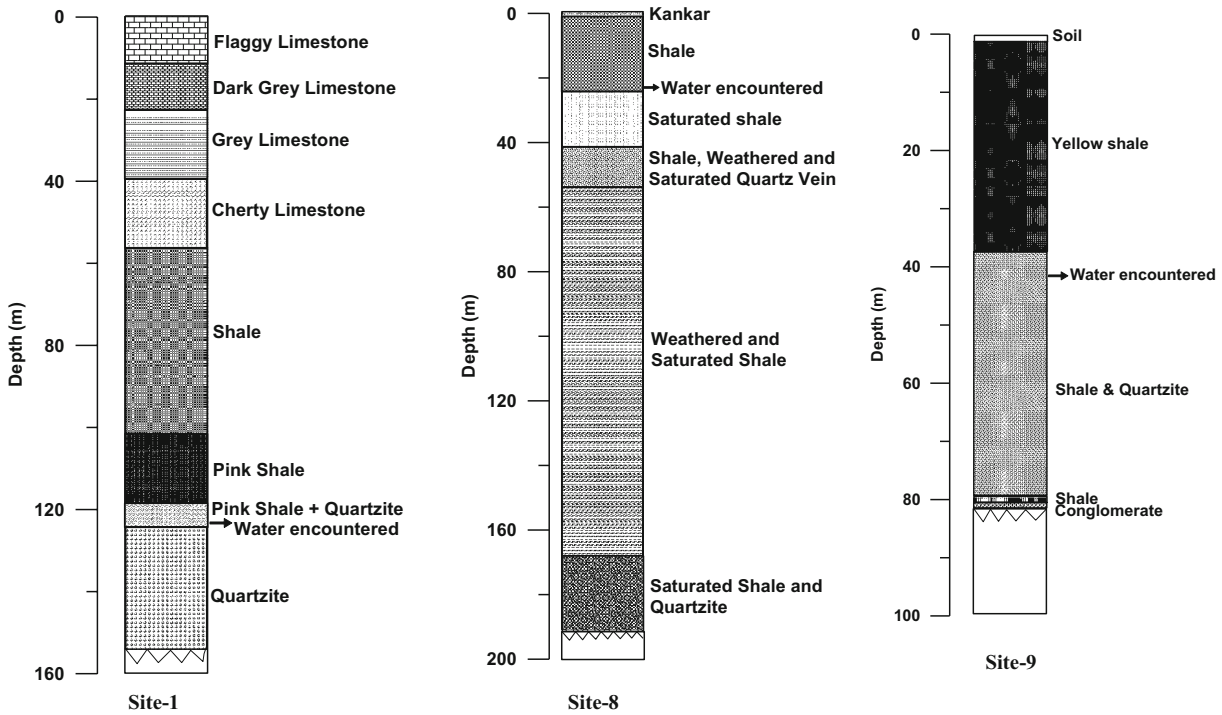

Figure 8. Detailed lithology of the drilled boreholes namely at site-1, 8 and 9 and its validation showing the water encountered at the contact zone(s) of shale and quartzite rocks as well as in the weathered shale formation.

formations. The marked drilling points were confirmed by the borehole drilling and thus validated the results of the respective high resolution electrical resistivity models. The depths of the top of the aquifer zone in these boreholes vary from 24 to 124 m depth bgl while the depth of the boreholes ranges from 81 to 192 m depths (figure 8). The details of the boreholes drilled are presented in table 1, and their specific lithology for the drilled sites 1, 8 and 9 are depicted in figure 8.

6.7 *Pumping tests of drilled boreholes for aquifer characterization*

The aquifer in the area is considered to be confined without boundary effect. This is based on available information on the regional hydrogeology of the area. The new lithological data shows that the aquifer zones were met in shales or at the contact zone of shale–quartzite formation. Pumping tests is the key to understand the aquifer health and its performance for any hydrogeological setting in any geological condition. To ascertain the groundwater potential in any area, and to evaluate the impact of pumping on the groundwater system, it is cardinal to know the aquifer parameters namely, transmissivity (T) and storage coefficient (S) for aquifer characterization. These aquifer parameters are also crucial for the management of the groundwater resources through the application of groundwater flow model.

Pumping tests are usually performed using a submersible pump and making the observation in the nearby observation well(s) and the pumping well. In the study area, the pumping tests were performed in four newly drilled boreholes with the prescribed standard procedure. Here, none of the boreholes have a nearby observation well that could have been used for observation of drawdown due to pumping. Hence, the drawdown and recovery data of pumping wells have been used for estimating the aquifer parameters in the present situation. Figure 9 shows drawdown-recovery curves for all the four boreholes. Based on the discharge measured at the time of drilling, a low discharge pump (2 HP) was installed in these boreholes for extraction of water. The discharge during the test was monitored at a regular interval of time. It was observed that the discharge rate was uniform throughout the pumping period. Water level indicators were used for monitoring the drawdown and recovery of the water levels in the boreholes. The pumping test data including pumping and recovery phase, have been interpreted considering the geological field conditions to

Table 1. *Details of the drilled boreholes with depth of the aquifer, water levels, etc.*

Borehole no.	Location	Lat., Long.	Depth of borehole (m)	Depth of top of aquifer zone (m)	Depth of submersible pump (m)	Static water levels (m)
1	Pit 1 near ERT-1	78.0613, 15.0583	154.0	124.0	132	18.14
8	Sunkalamma temple near ERT-8	78.0523, 15.0391	192.0	24.0	30.48	7.66
9	Ayyavaripalle near ERT-9	78.0017, 15.0283	81.0	42.0	54.9	24.0
10	Pit 2, near ERT-10	78.0267, 15.0736	192.0	64.0	73.0	21.1

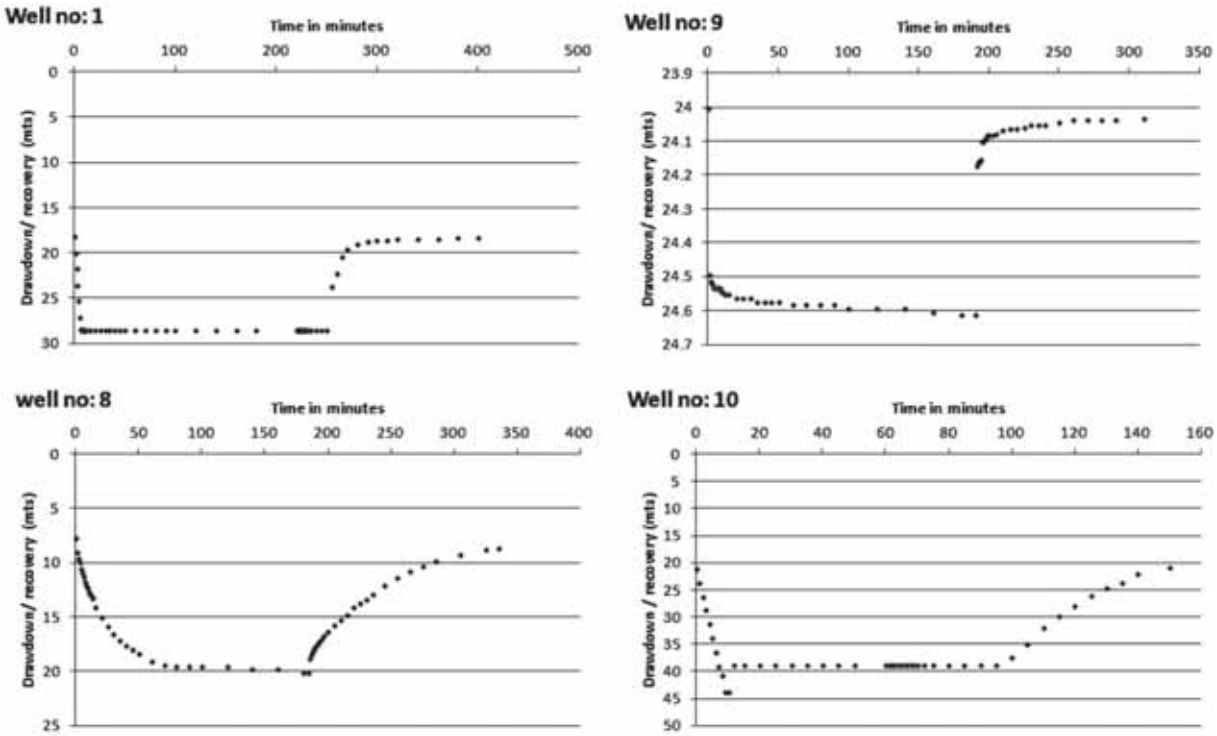

Figure 9. Drawdown and recovery curves of the four newly drilled boreholes in the area of study.

evaluate the aquifer parameters. A numerical method as described by Singh (2000), was used to interpret the pumping test data considering both pumpings as well as recovery phase.

Time–drawdown and recovery curves field data (figure 9) for each site were obtained from the pumping test analysis. The interpretation leads to the estimation of the aquifer parameters is presented in table 2. The transmissivity values have been found to vary from 0.292 to 179.5 m^2/d and based on these results of the pumping tests the boreholes at site-1, 8 and 9 have been used for supply of water for a long term while borehole at site-10 for a short term supply of water within the study area in the present complex geological settings.

7. Discussion

The large data density 2D inverted resistivity models revealed the most prospect groundwater scenario at three sites namely at Tummalapenta, Ayyavaripalle and Guruvanipalle, with the variation in aquifer depths and yields. The drilling at these three sites was very exciting and significant due to a large variation in resistivity contrast ranging from $\sim$20 to 2.75 $\times 10^5$ Ωm with respect to the surrounding rocks and the depth of the geological formations. The resistivity models in association with the borehole lithologies and the geological models had confirmed that the lowest resistivity range corresponds to shale while the highest resistivity value represents the massive quartzite

Table 2. *Aquifer parameters estimated through pumping tests from the newly drilled boreholes.*

Borehole no.	Pumping duration (minutes)	Initial and final water level (m)	Discharge rate m^3/d	Transmissivity estimated in m^2/d (based on drawdown data)	Transmissivity estimated in m^2/d (based on recovery data)	Average Transmissivity m^2/d	Storage coefficient estimated
1	220	18.14/28.55	I hr: 69.1 II hr: 66.5 III hr: 60.7 av: 65.4	0.997	1.67	1.33	0.237
8	185	7.66/20.07	I hr: 77.3 II hr: 75.4 III hr: 75.6 av: 76.1	2.31	2.54	2.42	0.5
9	190	24.00/24.61	I hr: 69.1 II hr: 66.5 III hr: 60.7 av: 65.4	181.0	178.0	179.5	
10	60	21.1/38.8	I hr: 47.5 II hr: 27.6 III hr: 18.7 av: 31.2	0.3	0.285	0.292	0.137

formation. Nevertheless, these three sites among all the others have depicted the highest anomalous nature in terms of physical property for groundwater exploration and prospecting in the present hydrogeological condition. The inverse resistivity structure at Tummalapenta (site-1) depicted a low resistivity zone with a resistivity value between ∼20–150 Ωm towards the southern side of the resistivity section. A major fault (**F–F**) is mapped and delineated from resistivity tomography inverted model towards the southern side of the profile, and this fault structure separated between the low resistivity 100–200 Ωm and the high resistivity $>17\times10^3$ Ωm geological formations. The fault, which is extended up to 230 m depth, is the potential target for groundwater exploration and prospecting all along the fault plane and towards the southern side. However, there is no prospect for groundwater towards the northern side of the fault, which is a highly massive and resistive formation with the resistivity of the order ranging from 70,443 to 274,770 Ωm. The potentiality for groundwater of the inferred fault was confirmed by a borehole drilling at this site up to 154 m depth, which encountered groundwater at a depth of 124 m bgl at the contact of shale and quartzite rock formation. Once the borehole was settled, the static water level measured is at 18.14 m bgl and is under unconfined condition. This is unique and a new finding delineated both the sedimentary rock (shale) as well as metamorphic rock (quartzite), where these two classes of rock have a wide range of resistivity variation and a very distinct hydrogeological property (figure 3, site-1). The conceptual geological model (site-1) explains and illustrates the geological sequences/cross-section of various rock formations, delineated the major fault structure and the implication for the availability of deeper groundwater resources. The 2D inverted resistivity model at another location in Tummalapenta (site-8) inferred groundwater potential zone towards SW direction located between lateral distances 500–640 m in the depth range 110–180 m. Here, the resistivity structure revealed a massive rock formation towards NE direction of the resistivity model (figure 4, site-8). The groundwater potential zone located towards the SW direction was confirmed and validated by a drilled borehole up to 192 m depth (figure 4a, b). The water encountered at a shallow depth of 24 m in the shale formation. The static water level measured is at 7.66 m bgl (figure 4, site-8 and table 1). The 2D inverted resistivity model result corroborated with the lithology of the drilled borehole and confirmed the presence of shale and quartzite formation (figures 4 and 8, site-8). The resistivity of the shale formation, which is achieved at a depth of 24 m is close to 1150–1180 Ωm and this value of resistivity matches with the modelled resistivity (figure 4). Further down 24 m depth in the borehole, it was found the saturated shale with slightly more compactness, which corroborates with the resistivity model structure

(figures 4 and 8, site-8). This is followed by shale, weathered and saturated quartz vein as depicted in the borehole lithology (figure 8, site-8). Subsequently, it was found weathered and saturated shale formation of 115 m thick zone from the borehole lithology. At a deeper 168.5 m depth it encountered saturated shale and quartzite formation and it continues until 192 m depth (figures 4 and 8, site-8), which is the major aquifer zone in the shale and quartzite formation. This saturated shale and quartzite formation depicted a low resistivity zone ∼100–450 Ωm as revealed from the resistivity model result (figure 4a), which corroborated with the borehole lithology at this site (figure 4b). Likewise the inverse model resistivity structure at Ayyavaripalle (site-9) depicted a relatively more prospect groundwater scenario in the eastern direction than in the west due to more intense weathered geological formations, which revealed a low resistivity (∼15–100 Ωm) values. The geological formation is highly weathered and fractured towards the eastern side with a resistivity contrast >300 Ωm up to 100 m depth. However, the high resistivity formation indicated the massive formation with a different degree of compactness and hardness showing resistivity in the range ∼300 to $\sim 18\times10^3$ Ωm. The groundwater prospect zone lies at a shallower depth between 30–100 m depth on the eastern side of the resistivity model. This groundwater zone with a resistivity value ∼15 to <100 Ωm, which is located between 540–620 m lateral distance towards the east is hydrogeologically the favourable and prospect aquifer zone for groundwater exploration, prospecting and development in the varied hydrogeological setting. This resistivity result was validated by a drilled borehole up to 81 m depth at the anomalous potential target towards east and the water encountered at a depth of 42 m near the contact of shale and weathered quartzite zone. The static water level was measured and found at a depth of 24.0 m bgl at Ayyavaripalle site (figure 7). The lithology of the borehole at this site encountered soil layer, shale, shale and quartzite and then shale, conglomerate in the entire lithology section until 81 m depth (refer figures 7 and 8; site-9). On the other hand, the 2D inverted resistivity model at Guruvanipalle (site-10) shows a large resistivity contrast of the subsurface formations ranging from ∼10 to $\sim 70\times10^3$ Ωm all along the entire resistivity section (figure 6). In the southern side between 480 and 640 m lateral distance, a clear visible, highly anomalous wider groundwater prospect zone is inferred with a resistivity value between ∼15 and 150 Ωm. The host rock as revealed from the inverted resistivity model is highly weathered/fractured and inferred as saturated formation on the southern side, while it is comparatively much harder geological formation on the northern side of the resistivity section (figure 6). The groundwater prospect zone is very much prominent from ∼35 m up to 200 m depth within the anomalous low resistivity zone and it was confirmed by a drilled borehole up to a depth of 192 m. The water encountered at 64 m depth (figure 6, table 1). This unique findings through high resolution resistivity model result clearly depicted that the areal extent of this anomalous zone extends from ∼35 m to the deepest 200 m depth with a resistivity contrast of ∼200 Ωm. The static water level measured is at 21.1 m bgl at this drilled borehole location (figure 6, table 1). This detailed study exemplify the high resolution resistivity models with prominent and anomalous results in terms of hydrogeology, which are confirmed by drilled boreholes up to a maximum depth of 192 m at four prospect sites and these boreholes tapped the groundwater zones but with yields ranging from 300 to ∼5000 lph. This shows a wide variant in a water holding capacity in the subsurface geological strata within the complex sedimentary and hard rock formations, which constitutes limestone, shale and quartzite rock formations. Nevertheless, the groundwater reserves and quality can be improved through suitable artificial recharge means. At the same time, the storage structure in the northwestern part of the plant may be rejuvenated by desilting for improving the more storage of groundwater and thereby increasing recharge to the subsurface aquifer and thus leading to the optimal management of groundwater resources for future needs and demand. The high resolution electrical resistivity datasets and the lithology of the drilled boreholes together has immensely helped in realistic conceptualization and understanding of the aquifer system in the present variant geological setting as well as in another area of similar geological settings.

8. Conclusions

Based on 2D geophysical investigation and hydrogeological data in the complex geological terrain, the following conclusions are drawn:

- Provided clear picture of the subsurface geological formations and structure with a large

variation in resistivity ranging from ∼20 to 2.75×10^5 Ωm.
- The modelled resistivity values corroborated with the borehole lithology viz., for limestone, shale and quartzite formations and thus it is a new finding where the high resolution electrical resistivity results had delineated distinctly the above said three formations.
- The 2D resistivity models, lithology obtained from the drilled boreholes and the geological models together had helped in detailed understanding of the aquifer and the hydrogeology of the area.
- Delineated four prospect aquifer zones with low to moderate potential, which was confirmed by borehole drilling with depths varying from 81 to 192 m.
- The depth to top of the aquifer zone lies between 24 and 124 m mainly at the contact zones of shale and quartzite rocks as well as in the weathered shale formation in the present geological setting of the area.
- The static water level varies from 7.66 to 24.0 m bgl within a small area reflecting a large groundwater dynamic change within the aquifer system. Regular monitoring of water levels show that the aquifer is connected to a recharge source.
- The aquifer transmissivity varies from 0.3 to 179.5 m^2/d, and their storage coefficient varies from 1.37×10^{-1} to 5×10^{-1}, which was used for both long and short term water supply.

Acknowledgements

Authors are grateful to Dr V M Tiwari, Director, CSIR–National Geophysical Research Institute, Hyderabad, India, for his kind permission and encouragement for carrying out the scientific work for research and development as well as of societal importance and bringing out this research paper. We are thankful to Mr G M Krishna, Unit Head and Mr T V Sreenivasan, Senior Vice President (Mines) of M/s Ultra Tech Cement Limited–APCW, Tadipatri, Andhra Pradesh, India for financially supporting the project study, their cordial help and necessary logistics during the investigations and geophysical survey. We acknowledge the help rendered by Shri M Srinivasulu and Mr K Srinivasa Rao, Geologists for their valuable interactions and discussion on the existing dataset and details about the area during the investigations. First author thanks, Dr S Thiagarajan for drawing and preparing the lithology of the drilled boreholes. The CSIR–NGRI reference number of the manuscript is NGRI/Lib/2018/Pub-31. We are highly benefitted with the comments and suggestions by the anonymous reviewers, which helped immensely to improve the quality of the paper.

References

Abdulaziz A M, Hurtado J M and Faid A 2012 Hydrogeological characterization of Gold Valley: An investigation of precipitation recharge in an intermountain basin in the Death Valley region, California, USA; *Hydrogeol. J.* **20(4)** 701–718.

ABEM 2012 ABEM Instruction Manual – Terrameter LS, 2012, 110p.

Adepelumi A A, Yi M J, Kim J H, Ako B D and Son J S 2006 Integration of surface geophysical methods for fracture detection in crystalline bedrocks of southwestern Nigeria; *Hydrogeol. J.* **14** 1284–1306.

Aizebeokhai A P and Oyeyemi K D 2014 The use of the multiple-gradient array for geoelectrical resistivity and induced polarization imaging; *J. Appl. Geophys.* **111** 364–376.

Andrade R 2011 Intervention of Electrical Resistance Tomography (ERT) in resolving hydrological problems of a semi-arid granite terrain of southern India; *J. Geol. Soc. India* **78(4)** 337–344.

Balkaya C, Kalyoncuoğlu U Y, Özhanlı M, Merter G, Cakmak O and Güven I T 2018 Ground penetrating radar and electrical resistivity tomography studies in the biblical Pisidian Antioch city, southwest Anatolia; *Archaeol. Prospect.* **25** 285–300.

Barker R D 1992 A simple algorithm for electrical imaging of the subsurface; *First Break* **10** 53–62.

Bernard J 2003 Short note on the depth of investigation of electrical methods, Iris instruments, 8p.

Dahlin T 1996 2D Resistivity Surveying for Environmental and Engineering Applications; *First Break* **14** 275–283.

Dahlin T 2001 The development of DC resistivity imaging techniques; *Comput. Geosci.* **27** 1019–1029.

Dahlin T and Loke M H 1998 Resolution of 2D Wenner Resistivity Imaging as assessed by numerical modelling; *J. Appl. Geophys.* **38** 237–249.

Dahlin T and Zhou B 2006 Multiple-gradient array measurements for multichannel 2D resistivity imaging; *Near Surf. Geophys.* **4(2)** 113–123.

Daily W, Ramirez A, Binley A and Labrecque D 2004 Electrical Resistance Tomography; *Leading Edge* 438–442.

Demanet D, Pirard E, Renardy F and Jongmans D 2001 Application and processing of geophysical images for mapping faults; *Comput. Geosci.* **27** 1031– 1037.

Evjen H M 1938 Depth factors and resolving power of electrical measurements; *Geophysics* **3** 78–95.

Gokturkler G, Balkaya C, Erhan Z and Yurdakul A 2008 Investigation of a shallow alluvial aquifer using geoelectrical methods: A case from Turkey; *Environ. Geol.* **54** 1283–1290.

Griffiths D H and Barker R D 1993 Two-dimensional resistivity imaging and modeling in areas of complex geology; *J. Appl. Geophys.* **29** 211–226.

Griffiths D H and Turnbull J 1985 A Multi-Electrode Array for Resistivity Surveying; *First Break* **3** 16–20.

Griffiths D H, Turnbull J and Olayinka A I 1990 Two-Dimensional Resistivity Mapping with a computer controlled array; *First Break* **8** 121–129.

Gupta G, Patil J D, Maiti S, Erram V C, Pawar N J, Mahajan S H and Suryawanshi R A 2015 Electrical resistivity imaging for aquifer mapping over Chikotra basin, Kolhapur district, Maharashtra; *Environ. Earth Sci.* **73** 8125–8143.

Hossain D 2000 2D Electrical Imaging survey in hydrogeology, The Bangladesh; *J. Sediment. Res.* **18(1)** 57–66.

King W 1872 The Cuddapah and Kurnool formations in the Madras Presidency; *Mem. Geol. Survey India* **1872(i)** 1–346.

Kumar D 2012 Efficacy of Electrical Resistivity Tomography technique in mapping shallow subsurface anomaly; *J. Geol. Soc. India* **80(3)** 304–307.

Kumar D, Mondal S, Nandan M J, Harini P, Soma Sekhar B M V and Sen M K 2016a Two-Dimensional Electrical Resistivity Tomography (ERT) and Time Domain Induced Polarization (TDIP) study in hard rock for groundwater investigation: A case study at Choutuppal Telangana, India, *Arab. J. Geosci.* **9(5)** 1–15.

Kumar D, Shankar G B K, Mondal S, Venkatesam V, Sridhar K, Rao P N, Madhnure P and Rangarajan R 2016b Mapping lithology and assessing recharge characteristics in a granitic hard rock aquifer: Inference from 2D resistivity, induced polarization, tracer and moisture measurements; *J. Geol. Soc. India* **88(1)** 29–38.

Kumar D, Mondal S, Rajesh K and Rangarajan R 2015 Mapping subsurface hard and soft rock with complex geological terrain for groundwater prospecting in Tadipatri Mandal, Anantapur district, Andhra Pradesh, Technical Report No. NGRI-2015-GW-879 (unpublished).

Loke M H and Barker R D 1996 Rapid least-squares inversion of apparent resistivity pseudosections by a quasi-Newton method; *Geophys. Prospect.* **44(1)** 131–152.

Loke M H and Dahlin T 2002 A comparison of the Gauss–Newton and quasi-Newton methods in resistivity imaging inversion; *J. Appl. Geophys.* **49** 149–162.

Loke M H 2012a 2D and 3D Resistivity/IP inversion and forward modeling, Geotomo Software Penang, Malaysia.

Loke M H 2012b Tutorial: 2D and 3D electrical imaging surveys, 172p.

Oldenburg Douglas W and Li Yaoguo 1999 Estimating depth of investigation in dc resistivity and IP surveys; *Geophysics* **64(2**) 403–416.

Pucci S, Civico R, Villani F, Ricci T, Delcher E, Finizola A, Sapia V, De Martini P M, Pantosti D, Barde-Cabusson S, Brothelande E, Gusset R, Mezon C, Orefice S, Peltier A, Poret M, Torres L and Suski B 2016 Deep electrical resistivity tomography along the tectonically active Middle Aterno Valley (2009 L'Aquila earthquake area, central Italy); *Geophys. J. Int.* **207** 967–982.

Ritz M, Parisot J C, Diouf S, Beauvais A, Diome F and Niang M 1999 Electrical imaging of lateritic weathering mantles over granitic and metamorphic basement of eastern Senegal, West Africa; *J. Appl. Geophys.* **41** 335–344.

Robert T, Dassargues A, Brouyère S, Kaufmann O, Hallet V and Nguyen F 2011 Assessing the contribution of electrical resistivity tomography (ERT) and self-potential (SP) methods for a water well drilling program in fractured/karstified limestones; *J. Appl. Geophys.* **75** 42–53.

Roy A and Apparao A 1971 Depth of investigation in direct current methods; *Geophysics* **36(5)** 943–959.

Singh V S 2000 Well storage effect during pumping test in an aquifer of low permeability; *Hydrol. Sci. J.* **45(4)** 589–594.

Singh S C and Paramasivam K 2016 Regional Lithological Characterization through Resistivity Imaging in parts of Chhatarpur district of Madhya Pradesh, India, published by Aqua Foundation in proceedings of 10th World Aqua Congress – International Conference held during 24–25th November, 2016 at New Delhi, pp. 125–139.

Suzuki K, Toda S, Kusunoky K, Fujimitsu Y, Mogi T and Jomori A 2000 Case studies of electrical and electromagnetic methods applied to mapping active faults beneath the tick Quaternary; *Eng. Geol.* **56** 29–45.

Swileam G S, Shahin R R, Nasr H M and Essa K S 2019a Spatial variability assessment of Nile alluvial soils using electrical resistivity technique; *Eurasian J. Soil Sci.* **8(2)** 110–117.

Swileam G S, Shahin R R, Nasr H M and Essa K S 2019b Assessment of soil variability using electrical resistivity technique for normal alluvial soils, Egypt; *Plant Arch.* **19(1)** 905–912.

Telford W M, Geldart L P, Sheriff R E and Keys D A 1976 Applied Geophysics, Oxford and IBH Publ. Co. Pvt. Ltd., 860p.

Thiagarajan S, Rai S N, Kumar D and Manglik A 2018 Delineation of Groundwater Resources using Electrical Resistivity Tomography; *Arab. J. Geosci.* **11(9)** 1–16.

Ward S H 1990 Resistivity and induced polarization methods; In: *Geotech. and Environ. Geophys.*, Vol. 1, Review and Tutorial, pp. 147–189.

Corresponding editor: Arkoprovo Biswas